KSCE Journal of Civil Engineering (2023) 27(4):1535-1550
DOI 10.1007/s12205-023-1240-4

pISSN 1226-7988, eISSN 1976-3808
www.springer.com/12205

Geotechnical Engineering

Corrosion Resistance and Compressive Strength of Cemented Soil Mixed with Nano-Silica in Simulated Seawater Environment

Qingsheng Chen[a,b], Hongyu Zhang[a], Jianjun Ye[a], Gaoliang Tao[a], and Sanjay Nimbalkar[c]

[a]*School of Civil Engineering, Architecture and Environment, Hubei University of Technology, Wuhan, Hubei 430068, China*
[b]*Dept. of Civil and Environmental Engineering, National University of Singapore, 119077, Singapore*
[c]*School of Civil and Environmental Engineering, University of Technology Sydney (UTS), Ultimo NSW 2007, Australia*

ARTICLE HISTORY

Received 13 July 2022
Revised 11 November 2022
Accepted 30 January 2023
Published Online 3 March 2023

KEYWORDS

Cemented soil
Nano-SiO_2
Simulated seawater environment
Unconfined compressive strength
Elastic modulus

ABSTRACT

Cemented soil structures are frequently exposed to the corrosive environment of seawater for an extended period, severely affecting their interior structure and mechanical qualities. This study presents laboratory-based approach to investigate the effect of nano-SiO_2 on the structural and mechanical properties of cemented soil in a simulated seawater environment. The unconfined compressive strength (UCS), elastic modulus and other mechanical properties of cemented soil mixed with nano-SiO_2 and ordinary silicate cemented soil were evaluated. X-ray diffraction (XRD) and scanning electron microscopy (SEM) were used to deduce the crystalline composition and microstructure characteristics of the modified cemented soil. The results show that the addition of nano-SiO_2 greatly increased the compressive strength and corrosion resistance of the cemented soil. In a 3C (105% salinity) simulated saltwater curing environment, the compressive strength of the cemented soil containing 2% nano-SiO_2 increased by 86% and 158% at 30days and 60days, respectively. XRD and SEM showed that nano-SiO_2 enhanced the interface structure of cemented soil and increased the compactness of the cement-soil system. The current study demonstrates that nano-SiO_2 could considerably improve the mechanical characteristics and corrosion resistance of cemented soil when exposed to simulated seawater.

1. Introduction

Cemented soils, a mixture of Portland cement, soil (or aggregate) and water, are typically employed in the deep cement mixing method to strengthen and stabilize soft ground (Yang et al., 2011; Luo et al., 2018). Apart from being a technique for strengthening soft ground, cemented soil is also utilized in the construction of highway embankments, airport runways, simulated islands, and marine geotechnical structures (Chen, 2013; Kim et al., 2018; Yu et al., 2020). These structures are often corroded by seawater over long periods of time. Although various researchers have examined the mechanical properties, rheology properties, and durability of cemented soil in a variety of dimensions (Ke et al., 2020; Lu et al., 2020; Gołaszewska and Giergiczny, 2021), most of these studies have been conducted in the natural environment on land, omitting the influence of environmental factors on cemented soil. Most of the materials used in marine engineering construction adopt the principle of proximity. Marine soft soils are widely distributed in the coastal areas of China (Wu et al., 2018; Zhang et al., 2018; Yu et al., 2019). Due to its high water content, high porosity and low strength, it usually needs to be strengthened in engineering applications. Cement materials have become one of the most commonly used soil stabilizers due to their good engineering properties and relatively low cost (Du et al., 2019). The presence of corrosive ions such as Mg^{2+}, Cl^- and SO_4^{2-} in the ocean environment has had a major effect on the strength of cemented soils used in marine, coastal, and shoreline engineering (Marchand et al., 2002). Numerous academics have conducted research on the performance of cemented soil in the presence of seawater corrosion. Li et al. (2017) demonstrated that after 90 days of exposure to seawater, the compressive strength of cement mortars reduced due to ionic erosion, and that pure calcium aluminate cement mortars were more resistant to seawater erosion than plain silicate cement mortars. The decrease in

CORRESPONDENCE Jianjun Ye 715470323@qq.com School of Civil Engineering, Architecture and Environment, Hubei University of Technology, Wuhan, Hubei 430068, China

cement mortar strength is primarily due to the fact that in a sulphate environment, the hydroxide and calcium ions in the cemented soil specimen are easily decalcified, resulting in the dissolution of the silicate and C-S-H gels (Glasser et al., 2008). When magnesium ions are present in the solution, the sulphate and magnesium ions combine to form $Mg(OH)_2$, hydrotalcite-like M-A-H and M-S-H gels, resulting in increased solid (De Weerdt and Justnes, 2015). Yu et al. (2018) investigated that the deterioration mechanism of cemented soil in sodium sulphate solution and clear water environments through complete submersion and dry and wet cycles. The unfavorable impacts of the sea environment on cemented soils have posed significant structural, mechanical, and durability issues. As a result, research is required to enhance the mechanical characteristics and corrosion resistance of cemented soil used in offshore engineering projects.

Nanomaterials and technologies have been proclaimed the "most promising materials and technology of the twenty-first century", and numerous studies have successfully used nanomaterials to improve the mechanical characteristics of cemented soil (Li et al., 2004; Kooshafar and Madani, 2020). nano-SiO_2, nano-MgO, nano-TiO_2, carbon nanotubes, and nano-clay are all common cemented soil modification nanomaterials (Jo et al., 2007; Yao et al., 2020; Wang et al., 2021), with nano-SiO_2 being the most extensively investigated nanomaterial thus far. Small quantities of nano-SiO_2 particles have been reported to dramatically improve the mechanical characteristics of cement or concrete in the available literature (Shih et al., 2006). For example, Bahmani et al. (2014) discovered that when 0.4 percent nano-SiO_2 was mixed with 8% cement and merely 8% cement, the compressive strength of the soil rose by 85 percent. Puerto Suárez et al. (2020) found that adding 1% and 1.5% nano-SiO_2 increased the compressive strength of cement mortars by 70% and 106%, respectively. On the one hand, the addition of nano-SiO_2 thickens the cement paste, accelerating the setting process and increasing the early strength of the cemented soil; on the other hand, it strengthens the bond between solid particles and consumes more CH crystals, effectively improving the interface structure (Qing et al., 2007). Until yet, little work has been carried on the use of nanomaterials to improve cemented soil in marine conditions. While nano-SiO_2 can enhance the mechanical qualities of cemented soil, corrosive solutions such as seawater and sulphate must also be considered.

The purpose of this study is to investigate the effect of nano-SiO_2 on the structural and mechanical properties of cemented soil in a maritime environment. The present study is conducted in a simulated seawater environment to preserve the specimens and compare the compressive strength of cemented soil mixed with nano-SiO_2 and ordinary silicate cemented soil. Advanced analytical techniques such as X-ray diffraction (XRD) and scanning electron microscopy (SEM) are used to deduce the microstructural mechanism by which nano-SiO_2 improves cemented soil and to deduce the evolution of the changes in macroscopic mechanical properties. The chemical composition and microstructure of cemented soils due to addition of nano-SiO_2 are also studied.

2. Laboratory Investigation

2.1 Materials

This study mainly used silty clay, cement, nano-SiO_2 and sea salt prepared seawater to preparing cemented soil sample. P32.5 ordinary silicate cement manufactured by Wuhan Yangchun Cement Co. was used in this experiment. Marine soft soils are widely distributed in coastal areas of China, and the soft soils mainly comprising silty clay and clay (Wu et al., 2018; Zhang et al., 2018; Yu et al., 2019). So we chose silty clay for the basic soil. The soil was extracted from the foundation pit 15 m deep in Wuhan construction site and was brownish yellow after air drying. According to ASTM D4318-17e1 (2017), the plastic

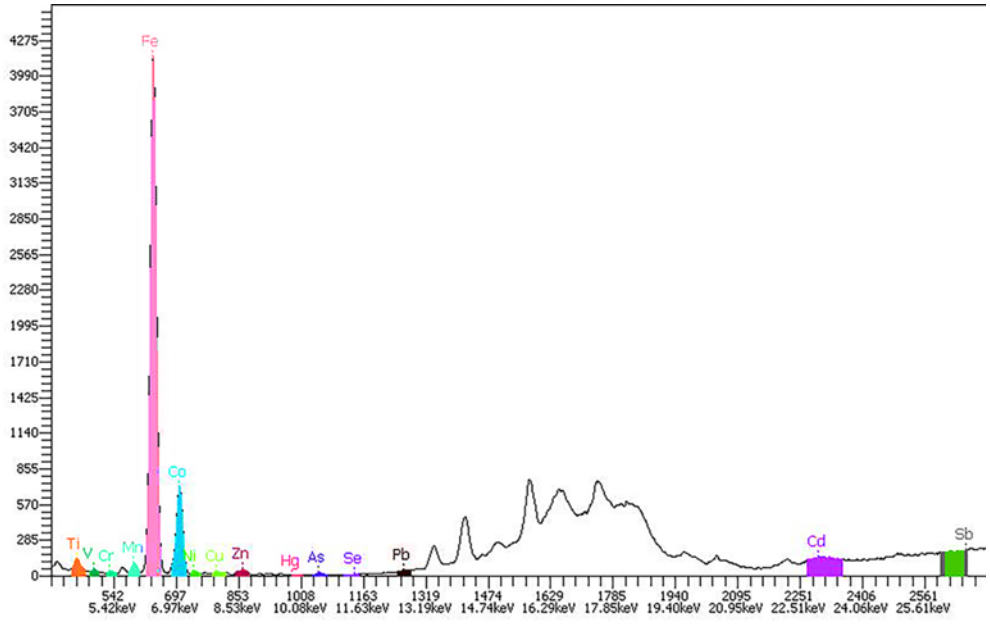

Fig. 1. Chemical Composition of the Silty Clay

Table 1. Characteristic Parameters of Nanomaterials

Category	Exterior	Grain Size (nm)	Specific Area (m^2/g)	Bulk Density (g/cm^3)	Purity (%)
Nano-SiO_2	White powder	25 – 35	190 – 250	0.057	99.5

Table 2. The Indicators of Each Ion Concentration between Simulated Seawater and Natural Seawater

Ion type	Cl^-	Na^+	SO_4^{2-}	Mg^{2+}	K^+	Ca^{2+}
Simulated Seawater (mg/L)	16,900 – 17,600	9,600 – 9.900	2,250 – 2,400	1,150 – 1,200	340 – 360	280 – 350
Natural Seawater (mg/L)	17,300 – 17,900	10,700 – 11,400	1,800 – 2,400	1,000 – 1,400	360 – 400	290 – 400

limit of the soil was determined to be 16.18% and the liquid limit to be 28.97% using a combined liquid-plastic limit tester, and the specific gravity was determined to be 2.77 using a specific gravity bottle test. The plasticity index is calculated as IP = WL (liquid limit) - WP (plastic limit). The plasticity index IP is calculated to be 12.79. According to the soil type classification, the soil utilized in this test was classified as silty clay. The soils used in this test are silty clay which are consistent with most of nature soft marine soils. The chemical composition of the silty clay was determined using an x-ray fluorescence (XRF) technique, with the highest elemental iron content. Fig. 1 shows the chemical composition of the silty clay.

Table 1 lists the intrinsic properties of the nano-SiO_2 employed in this study. Because the cost of shipping seawater was prohibitively high due to geographical constraints, this experiment used synthetic seawater composed of seawater pigments. According to Bin-Shafique et al. (2010), the average salinity of world marine saltwater is approximately 35‰, and this experiment created simulated seawater with a 35:1000 ratio of sea salt to water and a 1C = 35‰ concentration of seawater elements. In this study, 0C denotes a clean water environment, 1C denotes an simulated seawater environment with a salinity of 35‰, 2C denotes an simulated seawater environment with a salinity of 75‰, and 3C denotes an simulated seawater environment with a salinity of 105‰. In this paper, seawater concentration is denoted by C. At a room temperature of 22°C, the pH of the simulated seawater was 8.32. Table 2 shows that the ion concentration index of simulated seawater is comparable to that of natural seawater. The following is the process for preparing simulated seawater:

1. Weigh a specified mass of sea salt in an aluminium box using an electronic scale;
2. Take a 1L volumetric flask and pour the sea salt from the aluminium box into the flask;
3. Use a glass rod to introduce pure water into the volumetric flask, using the dropper when near the scale to ensure that the bottom of the concave surface of the solution coincides with the scale;
4. Stir the solution with a clean glass rod to dissolve the sea salt completely.

2.2 Mixing Ratio

Since the soil used in this test is free from salinity (i.e. sourced from an inland location), an simulated seawater was used to replicate the soft soil prevalent in the marine environment. According to Lee et al. (2005), the mixing ratio of cement mixed clay is expressed as *s:c:n:w*, *s* is the mass of dry soil, *c* is the mass of dry cement particles, *w* is the mass of simulated seawater, and $Aw = c/s$ is the amount of cement admixture. The test defined nano-SiO_2 as an admixture, *n* as the mass of nano-SiO_2 particles, $N_S = n/s$ as the nano-SiO_2 admixture, and $C_{wl} = w/(s + c + n)$ as the total simulated seawater content. The detailed mixing ratio of specimens for this test is shown in Table 3.

Table 3. Nano-Cement and Solid Mixing Ratio (%)

Number	N_S	S	Aw	Cw_1
1	0	100	15	50.22
2	1	100	15	50.67
3	2	100	15	51.12
4	3	100	15	51.57

2.3 Sample Preparation

The sample preparation using Nano-Silica is referred to the study of Lee et al. (2005) and Chen et al. (2022). The sample preparation using Nano-Silica is illustrated via different stages indicated below:

1. The silty clay was dried in an oven at 105°C and passed through a 2 mm sieve, and subsequently the soil was placed in a box and sealed for storage;
2. The dried clay particles, cement particles and Nano-Silica powder are combined according to the mixing ratios in Table 2 and then mixed well using a mixer with a continuous speed of approx. 2 min.
3. Add artificial seawater (according to the proportions in Table 2) and mix with a mixer for 5 min to mix the cement, Nano-Silica, clay and artificial seawater to a slurry state.
4. Poured the slurry into a cylindrical mold with a height of 80 mm and a diameter of 39 mm, and the air bubbles were discharged by shaking for 2 – 3 minutes on a vibrating table to dislodge air bubbles and ensure the specimen is dense.
5. Samples with air bubbles removed are placed in a constant temperature and humidity chamber for 48h.
6. After 48h of room temperature (20 – 24°C) cure, remove the mold and immerse the samples in artificially simulated seawater environment. Specimens were labeled and immersed in four different solution environments (clean water, 1C

simulated seawater, 2C simulated seawater, 3C simulated seawater) for 7 days, 28 days, 60 days and 90 days.

2.4 Unconfined Compressive Strength Test

The unconfined compressive strength test is equivalent to the special case where the circumferential pressure is absent in the case of a triaxial compression test.

According to the recommendation of Yang et al. (2020), the samples were vacuum saturated prior to conducting the UCS test to ensure that the saturation of all specimens was consistent. The test instrument is a model WE-100 universal testing machine with a range of 0 to 20 kN and a loading rate of 0 to 100 mm/min. The test was conducted at a rate of 1mm/min of axial compression. The average of the single compressive strengths of three parallel specimens at the same cement-to-solids ratio, curing age and curing environment is taken as a set of compressive strength values. If a specimen's compressive strength value deviates from the average value by more than 15% of the average value, the specimen's compressive strength value is disregarded. After completing the unconfined compression test, we crush the broken sample into powder. Dry the powder in a drying oven at 60ºC for later use.

The modulus of elasticity under different conservation environments was obtained according to Jiang et al. (2019). The results of the UCS test and the obtained elastic modulus values were used to analyze the effects of clear water and seawater environments on the macroscopic mechanical properties of the cemented soil.

2.5 X-Ray Diffraction Test

XRD is a technique for analyzing the atomic or molecular structure of a material. It is non-destructive and is most effective on fully or partially crystalline materials. The technique is often referred to as X-ray powder diffraction, because the material being analyzed is usually finely ground to a homogeneous state.

In order to investigate the corrosive effect of simulated seawater environment on the reactants and products of cemented soil and the improvement mechanism of nano-SiO_2 on the internal molecular structure of cemented soil, XRD tests were conducted. In the XRD test, we take the previously dried powder and place it on a glass slide for X-ray diffraction analysis. The instrument used in this XRD test was a polycrystalline X-ray diffraction analyzer with a diffraction angle of 10 – 80° and a diffraction rate of 10°/min. After concluding the test, the CH

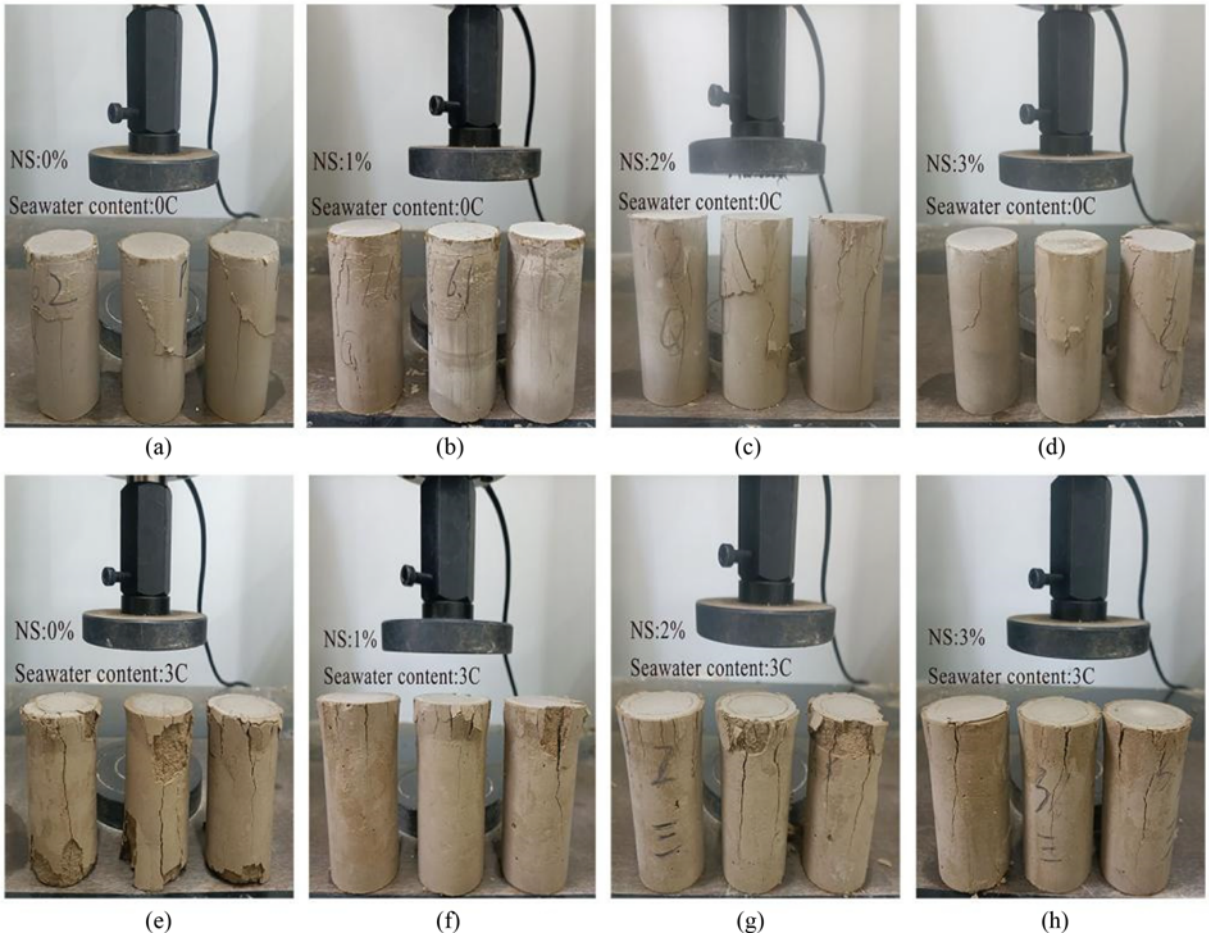

Fig. 2. Failure Specimens after the USC Test: (a) Seawater Content:0C; NS:0%, (b) Seawater Content:0C; NS:1%, (c) Seawater Content:0C, NS:2%, (d) Seawater Content:0C; NS:3%, (e) Seawater Content:3C; NS:0%, (f) Seawater Content:3C; NS:1%, (g) Seawater Content:3C, NS:2%, (h) Seawater Content:3C; NS:3%

crystal orientation at the end of the cement hydration reaction was obtained based on the study of Hussin and Poole (2011).

2.6 Scanning Electron Microscope Test

In order to reflect more visually the internal structural changes of the cemented soil after the modification of nano-SiO_2 and the erosion of simulated seawater, it was decided to conduct electron microscope scanning tests on the cemented soil specimens. Before conducting the SEM test, we need to pretreated the cemented soil specimen: take a flat specimen of cemented soil, carefully glue the specimen to the conductive adhesive and then vacuum dry the specimen. The vacuum dried specimens are then sputtered with gold. The purpose of the gold sputtering treatment is to ensure that the sample has good electrical conductivity so that the sample can be better viewed. The test was performed using a Hitachi SU8010 high-resolution field emission scanning electron microscope to observe the fine view morphology of the test pieces at different magnifications (500x, 5000x, 20000x).

3. Laboratory Results And Discussion

3.1 Unconfined Compressive Strength

3.1.1 Stress-Strain Curve

Figure 2 shows a picture of a universal testing machine crushing nano-SiO_2 cemented soil after immersion in water and seawater. NS in Fig. 2 indicates nano-SiO_2.

Figure 3 shows the stress-strain relationship curves of the UCS test of ordinary silicate cemented soil. As evident from Fig. 3, the peak strength of ordinary silicate cemented soil in clear water environment increase first and then decrease with the soaking time. The hydration of cement is a long-term process (Shihata and Baghdadi, 2001). Generally at 28 days the cement hydration reaction is 70 – 80% complete. During the initial period of seawater immersion (7 – 30 days), the increase in strength of the soil by the hydration reaction exceeds the increase in strength by the corrosion of the soil by the seawater; during the later period of seawater immersion (60 – 90 days), the corrosion of the soil

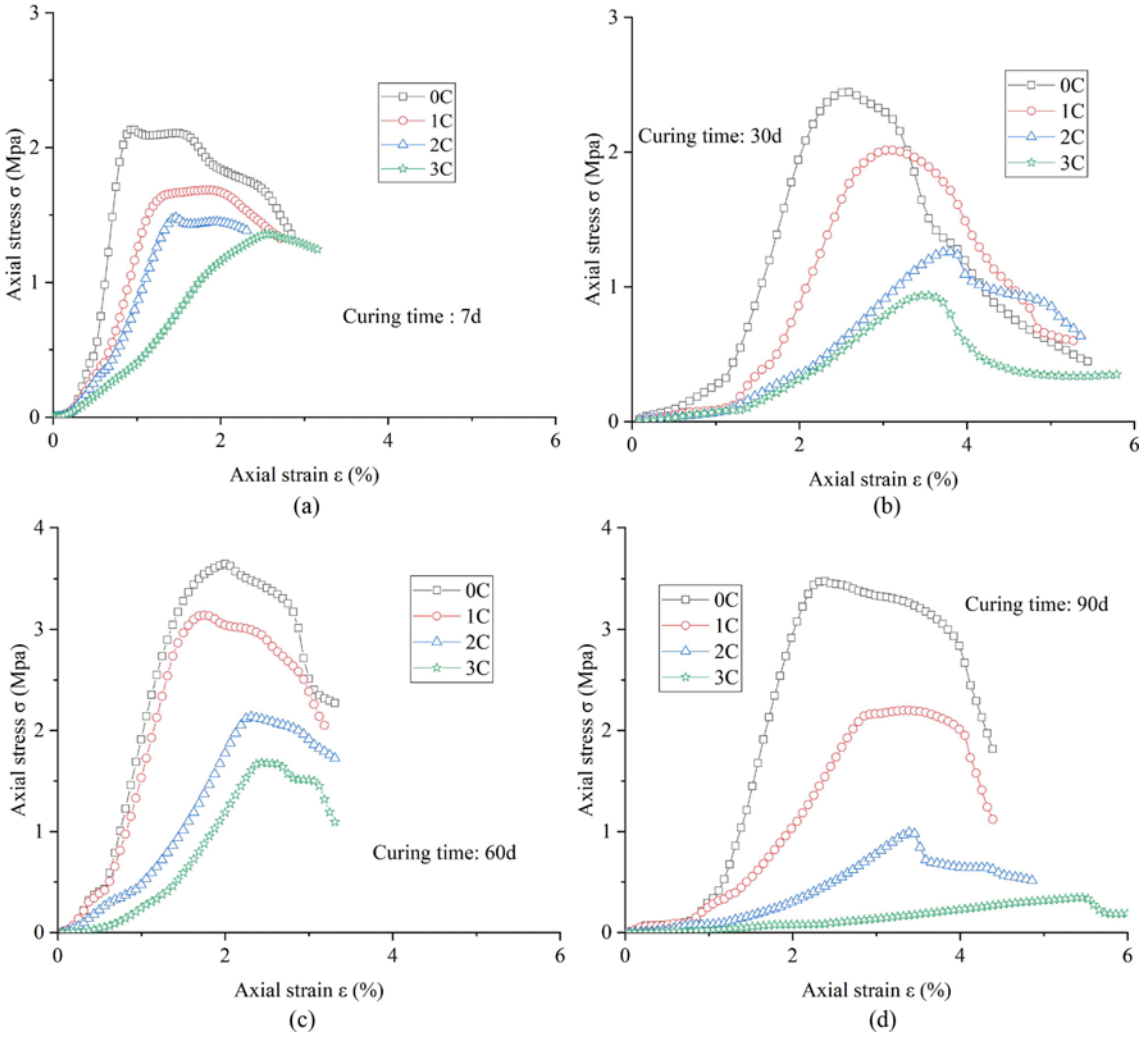

Fig. 3. Stress-Strain Curves of Ordinary Silicate Cement Soil Unconfined Compression Test: (a) Curing 7 Days, (b) Curing 30 Days, (c) Curing 60 Days, (d) Curing 90 Days

by the seawater gradually becomes stronger than the increase in strength by the hydration reaction. So the strength of the sample shows an increase and then a decrease with the increase of corrosion time. After 30 days of curing, the peak strength has a maximum value of 3.65 MPa. In simulated seawater environment, the higher the concentration of seawater, the more moderate the trend of stress-strain curve is observed for the conventional silicate cemented soil.

In the plasticity theory, if the stress increased with the increase of strain, but the rate of increase was slower and slower, and finally approaches a horizontal line, it was called strain hardening. If the stress increases with the increase of strain at the beginning, after reaching a peak value, the stress decreased with the increased of strain and eventually tends to be stable, which was called strain softening. According to the above analysis, the stress-strain curve of the cemented soil sample in Fig. 3 can be roughly divided into five stages:

1. In the initial stage, the stress increased gradually with the strain,
2. In the elastic deformation stage, the stress increased rapidly, and the stress-strain curve was approximately a straight line, which was because the cemented soil was subjected to further elastic deformation, and the initial micro-crack change of cement colloid has little effect,
3. In the plastic rising stage, the stress increased gradually and reached the peak,
4. In the strain-hardening stage, the stress does not decrease with increasing strain immediately after reaching its peak, and remains constant at its maximum value. At that time, the stress-strain curve is approximately a horizontal line, which indicates that the specimen is ductile deformation.
5. In the descending phase, the stress decreases gradually with increasing strain. At that time, the greater the slope of the decline of the stress-strain curve, the higher the strength of the cemented soil, but the poorer the ductility.

It is obvious from Fig. 3 that the slope of the elastic deformation phase decreases with the increase of the simulated seawater concentration and the peak intensity of the curve decreases. From these data, the longer the maintenance time in simulated seawater environment, the faster the rate of decline in the peak strength of ordinary silicate cemented soil, the worse the ability to resist seawater erosion. Thus, how to improve the corrosion resistance of ordinary silicate cement is a problem that needs to be solved in today's marine engineering practice.

Figure 4 shows the stress-strain relationship curves of the cemented soil after the addition of nano-SiO_2 at the curing age of 60 days. Combined with the stress-strain relationship curves, it can be found that only the 2% nano-SiO_2 doping amount of cemented soil shows strain hardening state in simulated seawater environment, which also indicates that the cemented soil with 2% nano-SiO_2 doping has good ductility and can produce certain deformation without damage.

In 1C simulated seawater environment, the peak strength of cemented soil with 2% nano-SiO_2 content was 4.52 Mpa, and the peak strength of cemented soil with 1% nano-SiO_2 content and 3% Nano-SiO_2 content was 4.39 Mpa and 4.38 Mpa, respectively. In

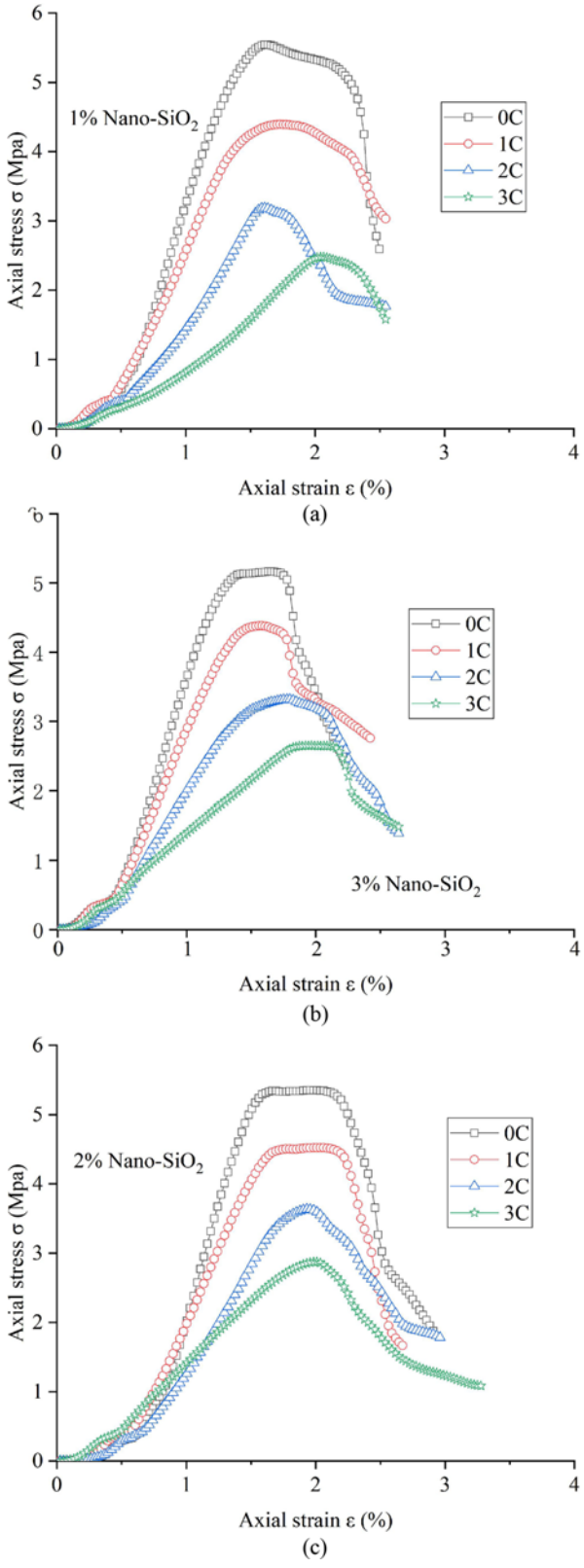

Fig. 4. Stress-Strain Curve of Nano-SiO_2 Cement Soil: (a) 1% Nano-SiO_2, (b) 2% Nano-SiO_2, (c) 3% Nano-SiO_2

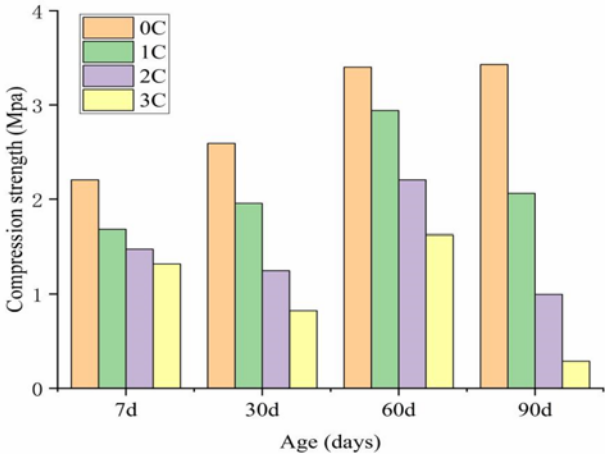

Fig. 5. Unconfined Compressive Strength of Ordinary Silicate Cement Soil

2C simulated seawater environment, the peak strength of cemented soil mixed with 1% and 3% nano-SiO_2 was 3.18 Mpa and 3.32 Mpa, respectively. In 3C simulated seawater environment, the peak strength of cemented soil with 1% and 3% nano-SiO_2 content was 2.87 Mpa and 2.64 Mpa, respectively. This indicated that the addition of nano-SiO_2 may make the cemented soil have better seawater corrosion resistance.

3.1.2 Compressive Strength

The average peak strength of three samples in each group was taken as the unconfined compressive strength (UCS) of cemented soil samples, and the UCS value was expressed by *qu*. Fig. 5 shows the relationship between UCS and curing days of ordinary silicate cemented soil in different curing environments.

The maximum UCS of ordinary silicate cemented soil was 3.4 Mpa in non-corrosive environment, that was, in clean water environment. Under different simulated seawater environments, the maximum compressive strength of ordinary silicate cemented soil was 2.9 Mpa, which was 15% lower than that under clean water environment, and the minimum compressive strength was 0.23 Mpa, which was 92% lower than that under clean water environment. It can be founded that under the same curing time, the UCS of ordinary silicate cemented soil decreases with the increase of simulated seawater concentration. The higher the simulated seawater concentration was, the more unfavorable the compressive strength of ordinary silicate cemented soil was. The possible cause of these situations might be due to the increased concentration of aggressive ions such as SO_4^{2-}, Cl^- and Mg^{2+} in the simulated seawater. The higher number of erosive ions has a more adverse effect on cemented soil structure, leading to a reduction in the compressive strength of cemented soil (Donatello et al., 2013).

It can be clearly seen from Fig. 6 that the compressive strength of nano-SiO_2 cemented soil was higher than that of ordinary silicate cemented soil in clear water. The highest compressive strength was 5.47 Mpa, which was 61% higher than that of ordinary silicate cemented soil.

The compressive strength of cemented soil with the same nano-SiO_2 content decreased with the increase of simulated seawater concentration, but the compressive strength value was higher than that of ordinary silicate cemented soil in simulated seawater environment. In this study, after 60 days of seawater corrosion the addition of 1%, 2% and 3% of nano-SiO_2 increased the UCS of the cemented soils by 51%, 55% and 52% respectively. In 1C simulated seawater environment, 2% nano-SiO_2 had the best effect among the three different nano-SiO_2 contents. In 2C and 3C simulated seawater environment, the compressive strength of 2% nano-SiO_2 to cemented soil was still the highest among the three different nano-SiO_2 cemented soil mixtures, which was 3.54 Mpa and 3.03 Mpa, respectively. Figs. 5 and 6 show that the nano-SiO_2 had a positive effect on the compressive strength of cemented soil and can improved the compressive strength of cemented soil to a certain extent. In the study of Qing et al. (2007), the addition of 1%, 2%, 3% and 5% of nano-SiO_2 increased the compressive strength of the cement paste by 20%, 21% , 23% and 25% respectively. Similar to the results of Qing et al. (2007), the addition of nano-SiO_2 improved the UCS of cemented soils. However, due to the different sample preparation methods and different solution environments the improvement efficiency of nano-SiO_2 in this study was significantly higher than that of Qing et al. (2007).

3.1.3 Seawater Corrosion Effect

In order to clarify the corrosion of cemented soil specimens by different seawater concentrations, the UCS loss rate *Fr* was set to reflect the reduction of compressive strength of cemented soil specimens under simulated seawater environment, and the effect of seawater corrosion on the mechanical properties of cemented soil is evaluated according to the magnitude of *Fr*. *Fr* can be calculated from Eq. (1):

$$F_r = \frac{q_{u0} - q_{ui}}{q_{u0}} \quad (i \in 1C, 2C, 3C). \tag{1}$$

Fr represented the unconfined compressive strength loss rate, q_{ui} was the compressive strength value of cemented soil sample under different seawater concentration, and q_{u0} was the compressive strength value of cemented soil sample under clean water environment. The results obtained by Eq. (1) were plotted in Fig. 7.

The larger *Fr* was, the stronger the corrosion effect of simulated seawater on cemented soil sample was. It can be seen from Fig. 7 that in 1C simulated seawater environment, the *Fr* of ordinary silicate cemented soil was 25% at the maintenance age of 30 days, and the *Fr* is reduced to 10% after the addition of nano-SiO_2. In 2C and 3C simulated seawater environment, the *Fr* of ordinary silicate cemented soil was 27%-21% higher than that of nano-SiO_2 when curing for 30 days. The loss rate of compressive strength of cemented soil with nano-SiO_2 was greatly reduced compared with that of ordinary silicate cemented soil. This indicated that the addition of nano-SiO_2 can counteracted the corrosion of seawater to a certain extent. When the curing age was 90 days, the *Fr* of ordinary silicate cemented soil was 71%

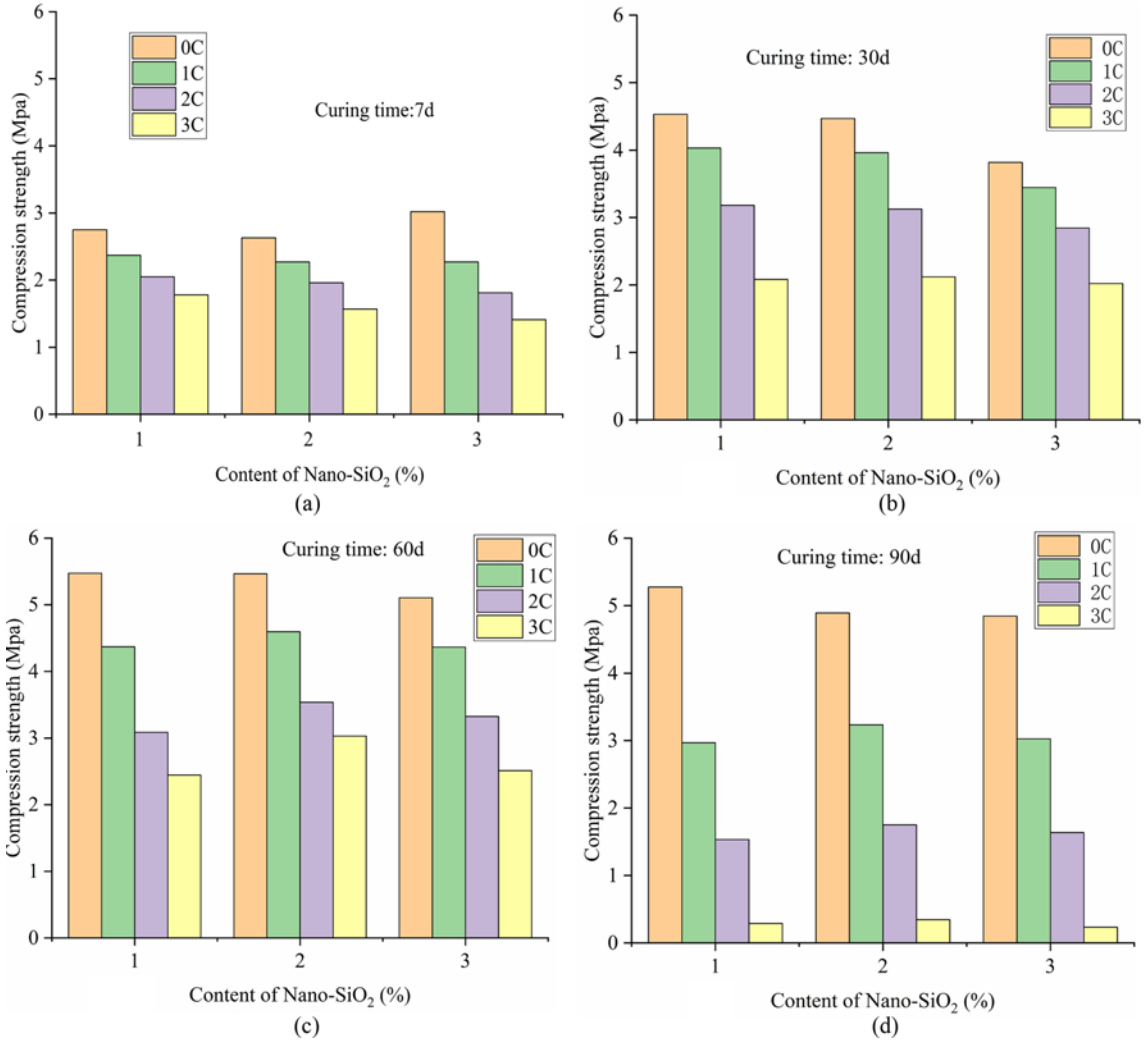

Fig. 6. Compressive Strength of Nano-SiO_2 Cement Soil: (a) Curing 7 Days, (b) Curing 30 Days, (c) Curing 60 Days, (d) Curing 90 Days

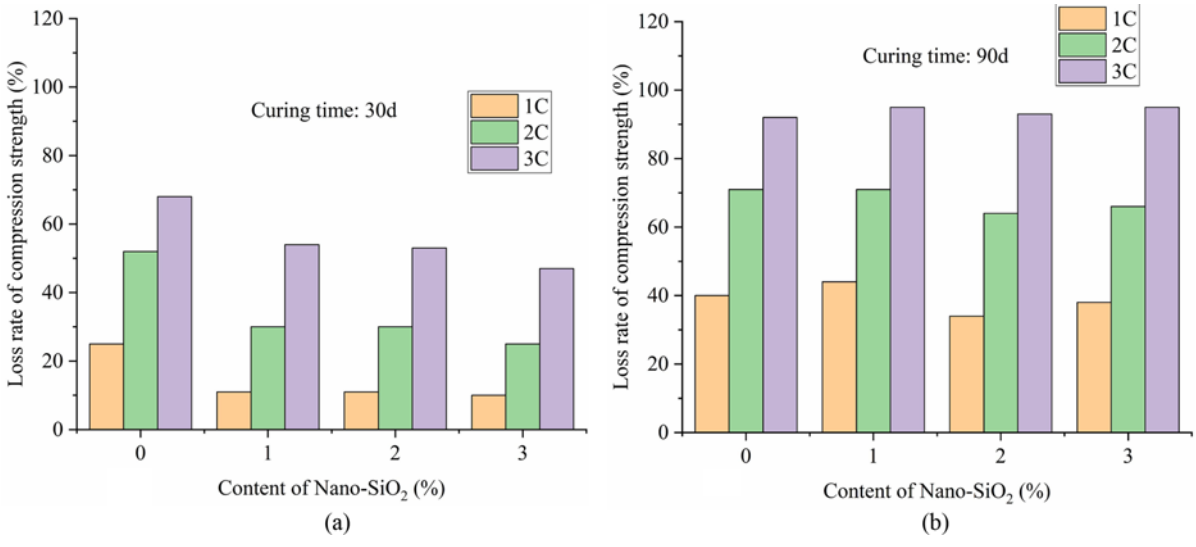

Fig. 7. Unconfined Compressive Strength Loss Rate: (a) Curing Time 30 Days, (b) Curing Time 90 Days

in 2C simulated seawater environment, and the *Fr* of nano-SiO_2 was 64% – 66%. However, in the 3C simulated seawater environment, the *Fr* of all cemented soil samples reached more than 90%. These data indicated that in the simulated seawater

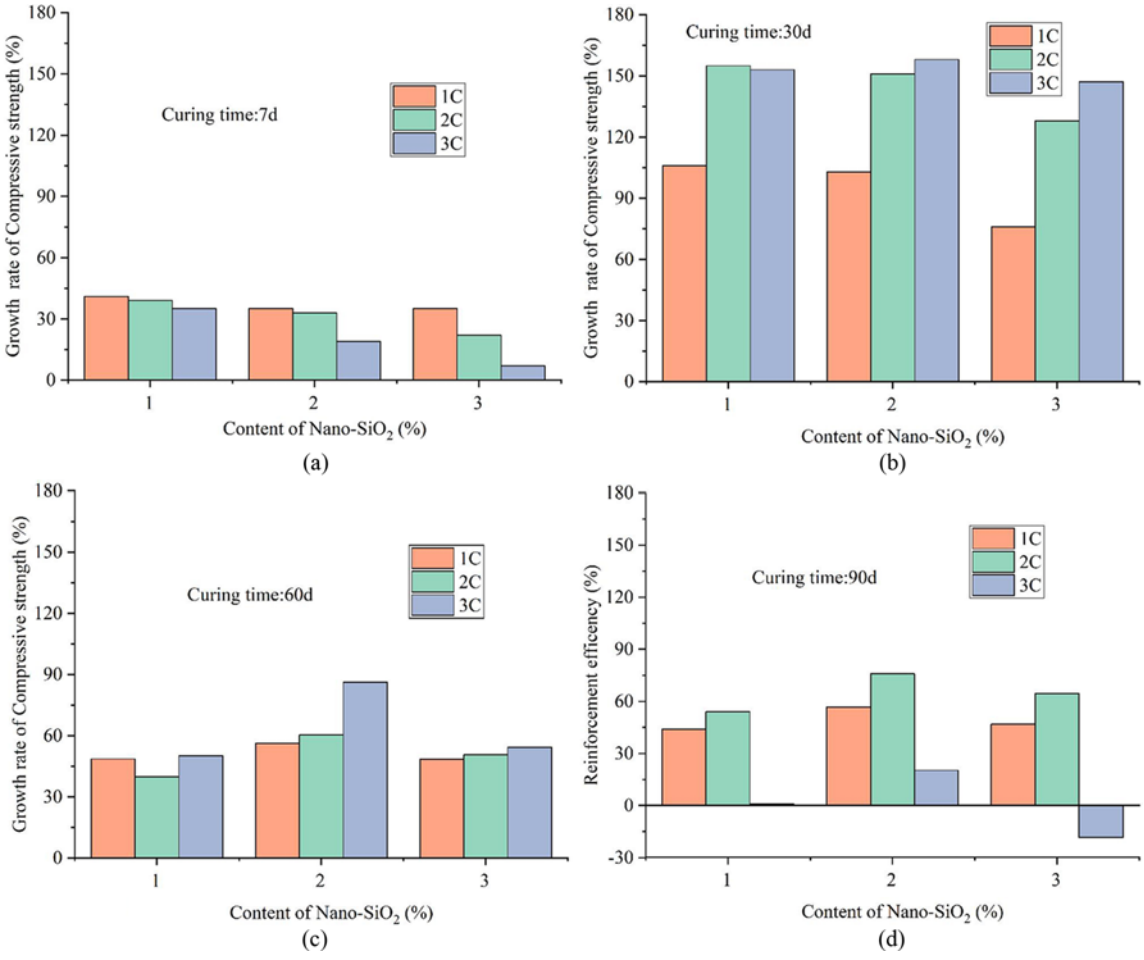

Fig. 8. Strength Growth Rate *Rs* of Cement Soil in Simulated Seawater Environment: (a) Curing 7 Days, (b) Curing 30 Days, (c) Curing 60 Days, (d) Curing 90 Days

environment with high concentration for a long time, the addition of nano-SiO_2 was difficult to offset the adverse effects of seawater corrosion. Simulated seawater environment generally has adverse effects on the compressive strength of cemented soil. The addition of nano-SiO_2 can only offset such effects to a certain extent, and the offset mechanism needs to be further discussed.

3.1.4 Improvement Effect of Nano-SiO_2

In order to reflect more intuitively the improvement effect of nano-SiO_2 on the cemented soil in seawater environment, the growth rate *Rs* of unconfined compressive strength is set to evaluate the mechanical effects of different doses of nano-SiO_2 on the cemented soil under the corrosive environment of seawater. *Rs* can be calculated from Eq. (2):

$$Rs = \frac{q_{uj} - q_{u1}}{q_{u1}} \quad (j \in N_S). \tag{2}$$

Rs represented the growth rate of unconfined compressive strength, q_{uj} represented the unconfined compressive strength of nano-SiO_2 cemented soil sample, and q_{u1} represented the unmeasured compressive strength of ordinary silicate Cemented soil. The values computed using Eq. (2) are plotted against nano-SiO_2 in Fig. 8.

Except the strength growth rate of 3% nano-SiO_2 cemented soil show in Fig. 8(d) was negative, Figs. 8(a), 8(b) and 8(c) shows that the nano-SiO_2 increased the compressive strength of cemented soil to a certain extent. The compressive strength growth rate of nano-SiO_2 cemented soil after curing for 30 days was extremely high. The highest 2% nano-SiO_2 cemented soil can reach 158%. Considered that most marine projects require long-term service life, combined with the engineering practice and the above analysis, it was founded that 2% nano-SiO_2 can improved the long-term corrosion resistance of cemented soil better than 1% and 3% nano-SiO_2. According to the research of Fu et al. (2020), The reason why the compressive strength of 3% nano-SiO_2 cemented soil is lower than that of 2% nano-SiO_2 may be due to the unstable internal structure of cemented soil caused by excessive nano-SiO_2.

The slope of the stress-strain curve (linear elastic portion of the stress-strain curve) is taken as the elastic modulus E_0 of the test sample, which can be obtained from Eq. (3) (Jiang et al., 2019):

$$E_0 = \frac{d\sigma(\varepsilon)}{d\varepsilon}\Big|_{\varepsilon=0}. \tag{3}$$

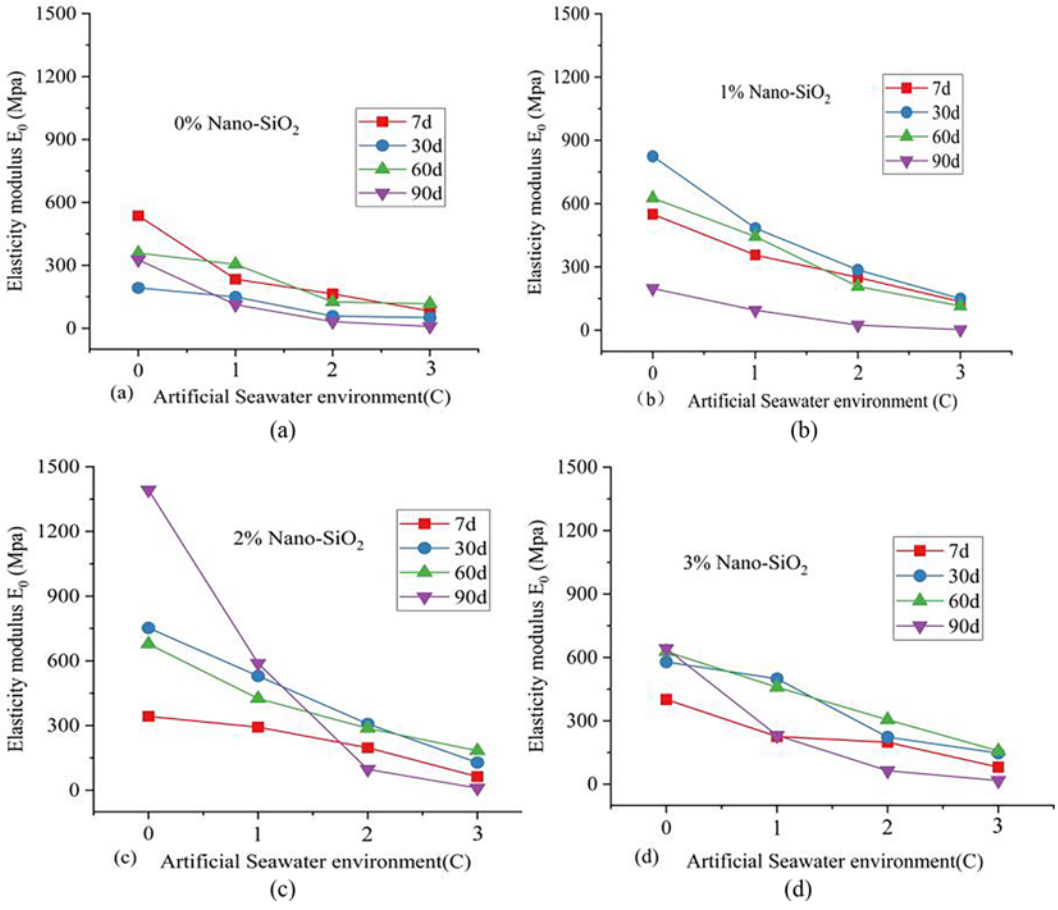

Fig. 9. Relationship between Elastic Modulus E_0 and Curing Environment: (a) 0% Nano-SiO_2, (b) 1% Nano-SiO_2, (c) 2% Nano-SiO_2, (d) 3% Nano-SiO_2

The stiffness of a material is usually measured by the elastic modulus E_0, and the greater the elastic modulus, the greater the stiffness of the material. The relationship between elastic modulus E_0 and different curing environments was shown in Fig. 9. According to the stress-strain relationship curve, the slope of the stress-strain curve at the elastic deformation stage was positively correlated with the peak strength of the same nano-SiO_2 powder content, that was, the larger the elastic modulus E_0 was, the larger the corresponding unconfined compressive strength was. It is evident from Fig. 9 that the elastic modulus decreased with the increase of seawater concentration. In a clear water environment, the elastic modulus of 2% nano-SiO_2 cemented soil sample reached 1392.1 Mpa, which is the highest among all cemented soil samples. Compared with other cemented soil samples, 2% nano-SiO_2 cemented soil samples have the largest elastic modulus of 588.6 Mpa and 97.2 Mpa, respectively, in a seawater corrosive environment of 1C and 2C for a long time (90 days). When the seawater concentration was the highest (3C), the elastic modulus of 2% nano-SiO_2 cemented soil sample was the highest, which was 183.3 Mpa. In conclusion, 2% as the best dosage of nano-SiO_2 in a long-term seawater corrosion environment, which was consistent with the analysis of the improvement effect of nano-SiO_2 on the unconfined compressive strength of cemented soil.

3.2 Scanning Electron Microscope Test

The excellent micro-structure and activity of nano-SiO_2 were the main reasons for improving the macroscopic mechanical properties of cemented soil. Scanning electron microscopy (SEM) tests were carried out on the surface of cemented soil samples which had been preserved for 7 days and 60 days respectively in the environment of clean water and seawater. The micro-structural characteristics of the samples after erosion were observed to analyze the improvement effect of nano-SiO_2 on cemented soil structure at the micro level. Figs. 10(a) and 10(b) shows the SEM images of ordinary cemented soil and nano-SiO_2 cemented soil preserved for 60d in clean water environment. Fig. 10 show the hexagonal lamellar $Ca(OH)_2$ crystals (CH) are evident. Calcium silicate hydrate (C-S-H) colloid are in reticular, colloidal or flocculent form; as well as columnar calcareous alumina (Aft) (Rajasekaran, 2005; Xing et al., 2009; Yang et al., 2012).

Figure 10(b) show that there are more columnar chalcocite and C-S-H colloid than Figs. 10(a), and the pores are also filled with nanoparticles to make the structure more densely. Although the CH crystals produced by cement hydration have high strength, they were easily affected by the environment and weak link of cemented soil (Fu et al., 2020). The reduction in the size of the CH crystals at the interface indicates that the interface structure has been improved, resulting in some increase in the

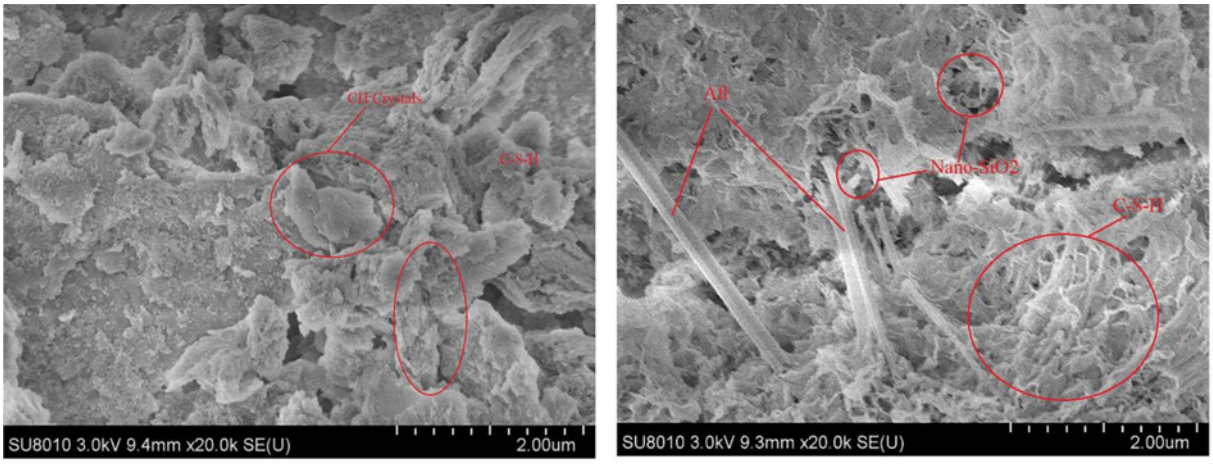

(a) (b)

Fig. 10. SEM Test Results of Ordinary Cement Soil and Nano-SiO_2 Cement Soil in Clean Water Environment: (a) Ordinary Cement Soil, (b) Nano-SiO_2 Cement Soil

unconfined compressive strength of the cemented soil. The main factor that enhances the compressive strength of cemented soil is that the hydration product C-S-H colloids exert an inter-structural bonding effect that tightly binds the soil particles and fills the pores (Lang et al., 2020). Calcareous alumina (Aft) is a hydration product, which was an expansive substance with low solubility, and can fill pores to a certain extent and improve the compressive strength of cemented soil.

Nano-SiO_2 can improve the microstructure of cemented soil in two aspects: on the one hand, the "filling effect" and "nucleation effect" of nano-SiO_2 fill the pores inside the soil sample structure, making the originally loose soil structure become compact; on the other hand, it is the "pozzolanic effect" of nano-SiO_2. The extremely small particle size of nano-SiO_2 gives it a huge surface energy. Such high surface energy can promote the reaction between nano-SiO_2 and cement hydration product CH crystal to generate more C-S-H colloid, thus improving the stability and compressive strength of cemented soil (Sobolev et al., 2009). By comparing Figs. 10(a) and 10(b), it was founded that C-S-H colloid increased after nano-SiO_2 was added, and a dense network structure was formed covering most cemented soil structures. Aft also increased significantly, forming a "bridge" between structures. As C-S-H colloid and Aft content increased, the chain of cement-treated soil and layered structure was further connected to form a whole nano-SiO_2 tiny size to fill the pore structure. This has further improved the coupling effects from these three cement-soil strength and stability, which is also reflected from identical results from unconfined compression test.

Figures 11(a) and 11(b) shows the SEM image of ordinary cemented soil and nano-SiO_2 cemented soil after curing for 60d in seawater environment. From the Figs. 11(a), the cracks of ordinary silicate cemented soil were very large in the environment of seawater erosion, and the structural connectivity was not enough, so it was in an extremely unstable state. Nano-SiO_2

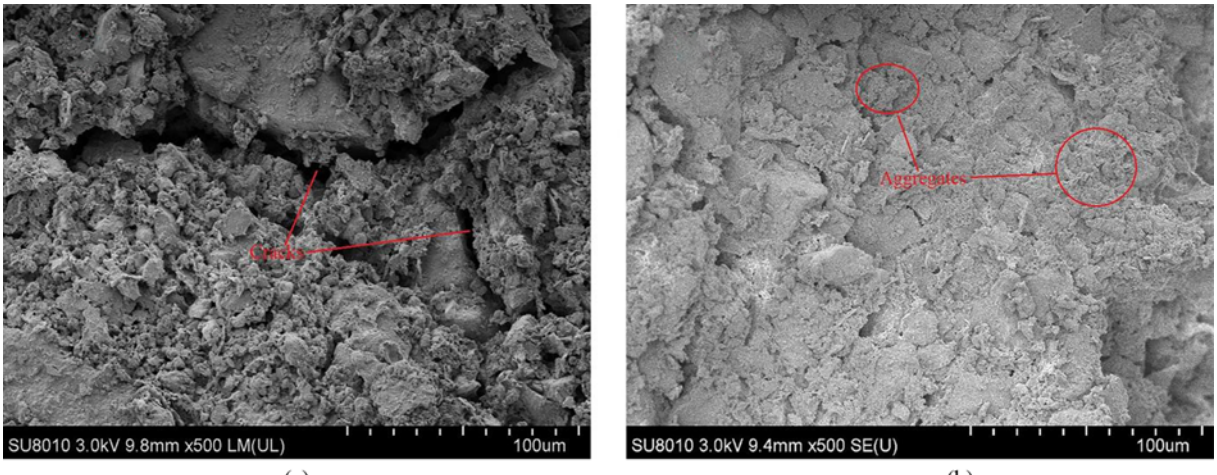

(a) (b)

Fig. 11. SEM Test Results of Ordinary and Nano-SiO_2 Cement Soil in Simulated Seawater Environment: (a) Ordinary Cement Soil, (b) Nano-SiO_2 Cement Soil

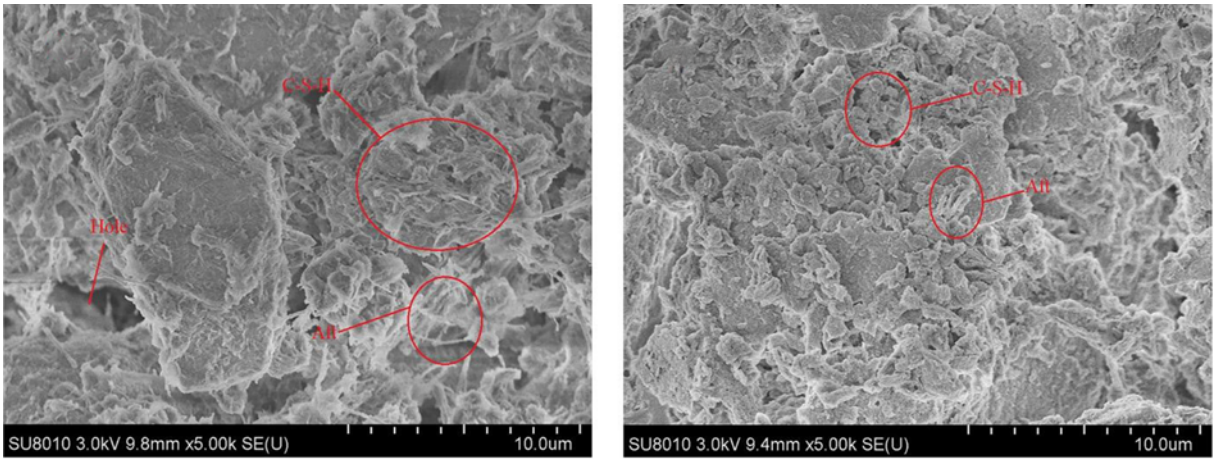

(a) (b)

Fig. 12. SEM Test Results of Nano-SiO_2 Cement Soil in Simulated Seawater Environment: (a) Curing 7 Days, (b) Curing 60 Days

cemented soil performed well without large cracks are shown in Figs. 11(b). There were many aggregates on the surface of soil particles, which improved the integrity of the cemented soil structure and made the structure more stable. This phenomenon indicated that the addition of nano-SiO_2 can effectively improving the microstructure of cemented soil in the seawater environment, thus improving the macro-mechanical properties of cemented soil (Liu et al., 2020).

Figures 12(a) and 12(b) shows the SEM images of nano-SiO_2 cemented soil curing for 7 days and 60 days respectively in 1C simulated seawater environment. Fig. 12(a) shows that the pores in nano-SiO_2 cemented soil structure become larger, C-S-H colloid no longer have a dense network structure after being corroded by seawater, but only covers the surface of soil particles very thin. Aft also becomes small and loses its "bridge" function, and the hydration reaction rate at this time was less than the erosion reaction rate. However, Fig. 12(b) show that the pores were filled with a large amount of C-S-H colloid, and Aft continued to act as a "bridge" between the structures, and there was much more C-S-H colloid than Aft at this time, indicating that the volcanic ash effect of SiO_2 nanoparticles became more and more obvious as time increased, and the rate of hydration reaction was greater than the rate of erosion reaction at this time.

Combining Figs. 6(c) with 10(d), conclude that the compression strength decreased at 90 days curing. After 60 days curing there would be difficult to create new CH crystal during the cement hydration reaction, and the original CH crystal would also be consumed due to the nano-SiO_2 "ash effect". As a result, the C-S-H colloid population no longer grows, but eventually declines due to environmental erosion. At this time, the erosion reaction rate was significantly greater than the hydration response rate, which was reflected in macroscopic mechanics as a decrease in compressive strength (Xing et al., 2009; Bahmani et al., 2014).

3.3 XRD Test

Ordinary silicate cemented soil and nano-SiO_2 cemented samples for 90 days were scanned respectively at the diffraction rate of 10°/min and the diffraction angle of 10° – 80°. The X-ray diffraction analysis results were shown in Fig. 13. Fig. 13 was the X-ray diffraction pattern of ordinary silicate cemented soil and nano-SiO_2 cemented soil samples in seawater environment and clean water environment after curing for 90 days.

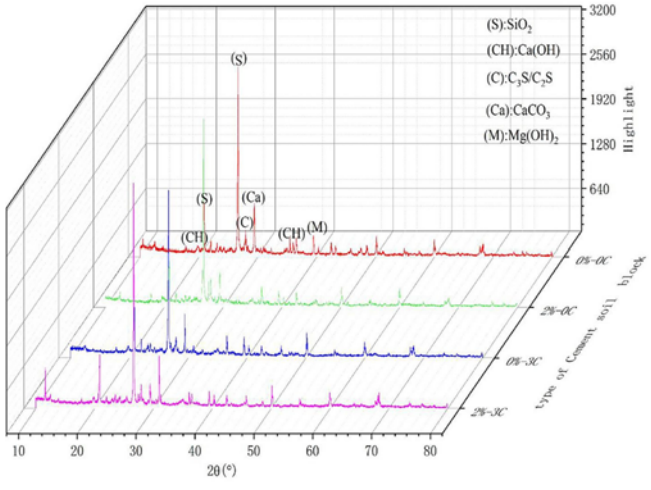

Fig. 13. X-Ray Diffraction Pattern of Cemented Soil Sample after Curing For 90 Days

According to the 2θ angle of different materials and the intensity of diffraction peak, the main crystal substances in cemented soil samples were analyzed and compared by semi-quantitative method. The diffraction peak angle of SiO_2 was 26.65°. CH crystal has two diffraction peak angles of 18.11° and 36.57° respectively. C_3S and C_2S react with water to form calcium silicate hydrate (C-S-H) colloid, and its diffraction angle is 27.95°; The diffraction angle of $CaCO_3$ was 29.48°. $Mg(OH)_2$ was formed by the reaction of C-S-H colloid with Mg^{2+} in seawater, and its diffraction angle was 39.47° (Fu et al., 2020). The diffraction peak intensity values of the raw materials and products of the chemical reaction are shown in Table 4.

Table 4. Diffraction Peak Intensity Values of Crystallites

Crystal Substance						
Group Name	SiO_2	Ca(OH)/001	Ca(OH)/101	$CaCO_3$	$Mg(OH)_2$	C_3S/C_2S
0%-0C	2,347	102	237	478	282	351
2%-0C	2,472	108	258	508	260	302
0%-3C	2,072	322	94	258	333	266
2%-3C	2,615	102	277	426	224	226

"0%-0C" in Fig. 13 and Table 4 refers to ordinary silicate cemented soil in a clear water environment. "2%-0C" was nano-SiO_2 cemented soil in clean water environment; "0-3C" was the ordinary silicate cemented soil under three times simulated seawater environment; "2%-3C" was nano-SiO_2 cemented soil under three times simulated seawater environment.

The reaction between SO_4^{2-}, simulated seawater and calcium carbonate leads to a reduction in the number of calcium carbonate crystals, resulting in lower diffraction intensity of calcium carbonate crystals in normal cemented soil than in nano-SiO_2 cemented soil. The reduction in the diffraction intensity of $CaCO_3$ crystals is one of the reasons for the decrease in the macroscopic mechanical properties of cemented soil (Rajasekaran, 2005). After 90 days of curing, the hydration reaction of cement has basically ended. C_3S and C_2S were the raw materials for hydration reaction, and their diffraction intensity decreased, indicated that the quantity of C_3S and C_2S was greatly consumed in cemented soil hydration reaction, that was, the hydration reaction is accelerated. The content of C_3S and C_2S in cemented soil decreased compared with ordinary silicate cemented soil after adding 2% nano-SiO_2, which indicated that the addition of nano-SiO_2 may greatly improve the efficiency of cemented hydration reaction.

$Mg(OH)_2$ was formed by the reaction of C-S-H colloid with Mg^{2+} in seawater (Fu et al., 2020). The content of $Mg(OH)_2$ decreased after the addition of nano-SiO_2 in a clear water environment, probably because Mg^{2+} could not easily enter the pores to react with C-S-H colloids after the addition of nano-SiO_2, so the content of $Mg(OH)_2$ decreased. The $Mg(OH)_2$ content of normal cemented soil is 15% higher in a seawater environment than in a clean water environment, probably due to the fact that Mg^{2+} in a seawater environment can more easily invade normal cemented soil to react with C-S-H colloids, thus reducing the number of C-S-H colloids and ultimately reducing the compressive strength of the cemented soil. This was consistent with the results of unconfined compressive strength test. From the experimental data, it can be founded that the $Mg(OH)_2$ content in seawater environment was significantly reduced after the addition of nano-SiO_2, even lower than that in clean water environment, which was likely to indicate that the addition of nano-SiO_2 significantly prevents the corrosive effect of Mg^{2+} in seawater.

CH crystal orientation was one of the important factors affecting cemented soil strength (Qing et al., 2007). According to Hussin and Poole (2011), for CH crystal, when (101) crystal plane was taken as the reference plane, the orientation index of (001) crystal plane was R, which can be obtained from Eq. (4):

$$R = \frac{1}{0.74}\left[I_{(001)} / I_{(101)}\right]. \tag{4}$$

Table 5. CH Crystal Orientation of Ordinary Silicate Cemented Soil and Nano-SiO_2 Cemented Soils at 90 Days Curing Age

Group name	$Ca(OH)_2$/001	$Ca(OH)_2$/101	R
0%-0C	102	237	0.581594252
2%-0C	108	258	0.565681961
0%-3C	322	94	1.686570291
2%-3C	102	277	0.497609523

CH crystal orientation of each group was shown in Table 5. As can be seen from Table 5, the orientation index R of ordinary silicate cemented soil is higher than that of nano-SiO_2 cemented soil. The greater the crystalline orientation, the poorer the interfacial structure of the cemented soil, resulting in weaker compressive strength (Fu et al., 2020). In 3C seawater environment, the crystal orientation of ordinary silicate cemented soil was the largest, reaching 1.69, which indicates that 3C seawater environment was extremely unfavorable to the compressive strength of ordinary silicate cemented soil. On the contrary, the CH crystal orientation of 2% nano-SiO_2 cemented soil decreased by 70.4%, indicating that in the same seawater environment, the addition of nano-SiO_2 may consume more CH crystals, reduce the size of CH crystals at the interface, and improve the interface structure of cemented soil more effectively, thus reducing the erosion effect of seawater on cemented soil. This is consistent with the research results of Qing et al. (2007).

In conclusion, the improvement of corrosion resistance and mechanical properties of cemented soil under seawater environment by nano-SiO_2 was the result of the comprehensive effect of filling effect, nucleation effect and pozzolanic effect.

4. Conclusions

This study presents laboratory-based approach to investigate the effect of nano-SiO_2 on the structural and mechanical properties of cemented soil in a simulated seawater appropriate to maritime environment. The unconfined compressive strength, elastic modulus and other mechanical properties of cemented soil mixed with nano-SiO_2 and ordinary silicate cemented soil were evaluated.

The micro-structural mechanism underlying the use of nano-SiO_2 for cemented soil improvement were also deduced by performing the X-ray diffraction (XRD) and scanning electron microscope (SEM) analyses. The experimental data support the following conclusions:

1. As the concentration of simulated seawater increased, the mechanical characteristics of cemented soil samples deteriorated, as evidenced by a drop in unconfined compressive strength. In a high concentration (3C) simulated seawater environment, the compressive strength of cemented soil deteriorated at a rate of up to 90%.
2. The inclusion of nano-SiO_2 significantly enhanced the mechanical properties of cemented soil in an simulated seawater environment, most notably the unconfined compressive strength. Nano-SiO_2 with a 2% concentration exhibited the highest rate of unconfined compressive strength improvement. As curing period of 30 and 60 days were used, its unconfined compressive strength rose by 86% and 158%, respectively, when compared to conventional silicate soil-based cement in a 3C simulated saltwater curing environment.
3. The enhancement of nano-SiO_2 on the microscopic level of cemented soil is primarily due to its superior filling and pozzolanic properties, which compact the structure of the cemented soil and improve the micro-structure, making it less susceptible to erosion by seawater ions, thereby increasing the unconfined compressive strength of cemented soil in the simulated maritime environment.
4. There are two main reasons why nano-SiO_2 enhances the compressive strength and corrosion resistance of the cement soil at the chemical reaction level. On the one hand, the addition of nano-SiO_2 accelerates the consumption of C_3S and C_2S in the reactants, prompting a substantial increase in the efficiency of the hydration reaction. On the other hand, the addition of nano-SiO_2 prevents the reaction of Mg^{2+} with C-S-H gel in the simulated seawater environment and reduces the loss of C-S-H gel, thus improving the corrosion resistance of the cement soil in the simulated seawater environment.

In summary, the current laboratory test results demonstrate that nano-SiO_2 is beneficial to the the compressive strength, elasticity modulus and microstructure of cemented soil when exposed to simulated seawater. In comparison to conventional silicate cemented soil, nano-SiO_2 cemented soil exhibited acceptable corrosion resistance and mechanical properties for the artificial seawater solution.

Acknowledgments

The research is financially supported by the National Natural Science Foundation of China (Grant No. 51978248).

Nomenclature

The following symbols are used in this paper:

Aw = Amount of cement admixture (unit: g)
C = Mass of dry cement particles (unit: g)
1C = Artificial seawater environment with a salinity of 35‰
C_{w1} = Total artificial seawater content (unit: %)
C_{w2} = Initial water content of the soil sample (unit: %)
E = Young's modulus (unit: Mpa)
E_0 = Elastic modulus (unit: Mpa)
Fr = Loss rate of q_u (unit: %)
IP = Plasticity index
N_S = Nano-SiO_2 admixture (unit: %)
q_u = Unconfined compressive strength (unit: Mpa)
q_{ui} = q_u of seawater concentration (unit: Mpa)
q_{uj} = q_u of nano-SiO_2 cement soil sample (unit: Mpa)
q_{u0} = q_u of clean water environment (unit: Mpa)
q_{u1} = q_u of ordinary silicate cement soil (unit: Mpa)
Rs = Growth rate of q_u (unit: %)
S = Mass of dry soil (unit: g)
W = Mass of artificial seawater (unit: g)
WL = Liquid limit (unit: %)
WP = Plastic limit (unit: %)
ε = Strain (unit: %)
σ = Stress (unit: Mpa)

ORCID

Not Applicable

References

ASTM D4318-17e1 (2017) Standard test methods for liquid limit, plastic limit, and plasticity index of soils. ASTM International, West Conshohocken, PA, USA

Bahmani SH, Huat BB, Asadi A, Farzadnia N (2014) Stabilization of residual soil using SiO_2 nanoparticles and cement. *Construction and Building Materials* 64:350-359, DOI: 10.1016/j.conbuildmat.2014.04.086

Bin-Shafique S, Rahman K, Yaykiran M, Azfar I (2010) The long-term performance of two fly ash stabilized fine-grained soil subbases. *Resources, Conservation and Recycling* 54(10):666-672, DOI: 10.1016/j.resconrec.2009.11.007

Chen K (2013) Reinforcement technology of cement agitation pile in the highway soft foundation treatment. *Applied Mechanics and Materials* 205-209, DOI: 10.4028/www.scientific.net/AMM.329.205

Chen Q, Yu R, Gaoliang T, Nimbalkar S (2022) Microstructure, strength and durability of nano-cemented soils under different seawater conditions: Laboratory study. *Acta Geotechnica* 1-21, DOI: 10.1007/s11440-022-01688-1

De Weerdt K, Justnes H (2015) The effect of sea water on the phase assemblage of hydrated cement paste. *Cement and Concrete Research* 55:215-222, DOI: 10.1016/j.cemconcomp.2014.09.006

Donatello S, Palomo A, Fernández-Jiménez A (2013) Durability of very high volume fly ash cement pastes and mortars in aggressive solutions. *Cement and Concrete Research* 38:12-20, DOI: 10.1016/j.cemconcomp.2013. 03.001

Du C, Yang G, Zhang T, Yang Q (2019) Multiscale study of the influence of promoters on low-plasticity clay stabilized with cement-based composites. *Construction and Building Materials* 213:537-548,

DOI: 10.1016/j.conbuildmat.2019.04.094

Fu C, Xie C, Liu J, Wei X, Wu D (2020) A comparative study on the effects of three nano-materials on the properties of cement-based composites. *Materials* 13(4):857, DOI: 10.3390/ma13040857

Glasser FP, Marchand J, Samson E (2008) Durability of concrete — Degradation phenomena involving detrimental chemical reactions. *Cement and Concrete Research* 38(2):226-246, DOI: 10.1016/j.cemconres.2007. 09.015

Gołaszewska M, Giergiczny Z (2021) Study of the properties of blended cements containing various types of slag cements and limestone powder. *Materials* 14(20):6072, DOI: 10.3390/ma14206072

Hussin A, Poole C (2011) Petrography evidence of the interfacial transition zone (ITZ) in the normal strength concrete containing granitic and limestone aggregates. *Construction and Building Materials* 25(5): 2298-2303, DOI: 10.1016/j.conbuildmat.2010.11.023

Jiang P, Mao T, Li N, Jia L, Zhang F, Wang W (2019) Characterization of short-term strength properties of fiber/cement-modified slurry. *Advances in Civil Engineering* 2019, DOI: 10.1155/2019/3789403

Jo BW, Kim CH, Tae GH, Park JB (2007) Characteristics of cement mortar with nano-SiO_2 particles. *Construction and Building Materials Abbreviations* 21(6):1351-1355, DOI: 10.1016/j.conbuildmat.2005.12.020

Ke G, Zhang J, Xie S, Pei T (2020) Rheological behavior of calcium sulfoaluminate cement paste with supplementary cementitious materials. *Construction and Building Materials* 243:118234, DOI: 10.1016/j.conbuildmat.2020. 118234

Kim AR, Chang I, Cho GC, Shim SH (2018) Strength and dynamic properties of cement-mixed Korean marine clays. *KSCE Journal of Civil Engineering* 22(4):1150-1161, DOI: 10.1007/s12205-017-1686-3

Kooshafar M, Madani H (2020) An investigation on the influence of nano silica morphology on the characteristics of cement composites. *Journal of Building Engineering Abbreviations* 30:101293, DOI: 10.1016/j.jobe.2020.101293

Lang L, Liu N, Chen B (2020) Investigation on the strength, durability and swelling of cement-solidified dredged sludge admixed fly ash and nano-SiO_2. *European Journal of Environmental and Civil Engineering* 1-21, DOI: 10.1080/19648189. 2020.1776160

Lee FH, Lee Y, Chew SH, Yong KY (2005) Strength and modulus of marine clay-cement mixes. *Journal of Geotechnical and Geoenvironmental Engineering* 131(2):178-186, DOI: 10.1061/(ASCE)1090-0241(2005)131:2(178)

Li G, Zhang A, Song Z, Shi C, Wang Y, Zhang J (2017) Study on the resistance to seawater corrosion of the cementitious systems containing ordinary Portland cement or/and calcium aluminate cement. *Construction and Building Materials* 157:852-859, DOI: 10.1016/j.conbuildmat.2017.09.175

Li H, Xiao H-g, Ou J-p (2004) A study on mechanical and pressure-sensitive properties of cement mortar with nanophase materials. *Cement and Concrete Research* 34(3):435-438, DOI: 10.1016/j.cemconres.2003.08.025

Lin R-S, Oh S, Du W, Wang X-Y (2022) Strengthening the performance of limestone-calcined clay cement (LC3) using nano silica. *Construction and Building Materials* 340:127723, DOI: 10.1016/j.conbuildmat.2022.127723

Liu X, Feng P, Shu X, Ran Q (2020) Effects of highly dispersed nano-SiO_2 on the microstructure development of cement pastes. *Materials and Structures* 53(1):1-12, DOI: 10.1617/s11527-019-1431-0

Lu J-X, Shen P, Zheng H, Zhan B, Ali HA, He P, Poon CS (2020) Synergetic recycling of waste glass and recycled aggregates in cement mortars: Physical, durability and microstructure performance. *Cement and Concrete Research* 113:103632, DOI: 10.1016/j.cemconcomp.2020.103632

Luo J, Liu X, Huang H, Luo J, Liu X, Huang H, Mi D, Chen D (2018) Mechanism analysis and application of cement-soil mixing pile in soft roadbed treatment. *Revue des Composites et des Matériaux Avancés* 28(2), DOI: 10.3166/RCMA.28.161-172

Marchand J, Samson E, Maltais Y, Lee RJ, Sahu S (2002) Predicting the performance of concrete structures exposed to chemically aggressive environment — field validation. *Materials and Structures* 35(10): 623-631, DOI: 10.1007/BF02480355

Murthy V (2002) Geotechnical engineering: Principles and practices of soil mechanics and foundation engineering. CRC Press

Puerto Suárez JD, Uribe CSL, Lizarazo-Marriaga J, Cárdenas-Pulido J (2020) Optimal nanosilica dosage in mortars and concretes subject to mechanical and durability solicitations. *European Journal of Environmental and Civil Engineering* 1-19, DOI: 10.1080/19648189.2020.1731715

Qing Y, Zenan Z, Deyu K, Rongshen C (2007) Influence of nano-SiO_2 addition on properties of hardened cement paste as compared with silica fume. *Construction and Building Materials* 21(3):539-545, DOI: 10.1016/j. conbuildmat.2005.09.001

Rajasekaran G (2005) Sulphate attack and ettringite formation in the lime and cement stabilized marine clays. *Ocean Engineering* 32(8-9):1133-1159, DOI: 10.1016/j.oceaneng.2004.08.012

Shih JY, Chang TP, Hsiao TC (2006) Effect of nanosilica on characterization of Portland cement composite. *Materials Science and Engineering* A424(1-2):266-274, DOI: 10.1016/j.msea.2006.03.010

Shihata SA, Baghdadi ZA (2001) Long-term strength and durability of soil cement. *Journal of Materials in Civil Engineering* 13(3):161-165, DOI: 10.1061/(ASCE)0899-1561(2001)13:3(161)

Sobolev K, Flores I, Torres-Martinez L, Valdez PL, Zarazua E, Cuellar EL (2009) Engineering of SiO_2 nanoparticles for optimal performance in nano cement-based materials. *Nanotechnology in Construction 3. Springer* 139-148, DOI: 10.1007/978-3-642-00980-8_18

Wang Y, Gu L, Zhao L (2021) Beneficial influence of nanoparticles on the strengths and microstructural properties of non-dispersible underwater concrete. *KSCE Journal of Civil Engineering* 25(11):4274-4284, DOI: 10.1007/s12205-021-1471-1

Wu Y-X, Lyu H-M, Shen JS, Arulrajah A (2018) Geological and hydrogeological environment in Tianjin with potential geohazards and groundwater control during excavation. *Environmental Earth Sciences* 77(10):1-17, DOI: 10.1007/s12665-018-7555-7

Xing H, Yang X, Xu C, Ye G (2009) Strength characteristics and mechanisms of salt-rich soil–cement. *Engineering Geology* 103(1-2):33-38, DOI: 10.1016/j.enggeo.2008.07.011

Yang XR, Zhang LY, Li HC, Dong LY (2011) Study and analysis on pile-soil stress ratio of the composite foundation of cement-soil mixing pile under flexible foundation. *Advanced Materials Research* 335:1145-1150, DOI: 10.4028/www.scientific.net/AMR.335-336.1145

Yang Y, Li S, Li C, Wu L, Yang L, Zhang P, Huang T (2020) Comprehensive laboratory evaluations and a proposed mix design procedure for cement-stabilized cohesive and granular soils. *Frontiers in Materials* 239, DOI: 10.3389/fmats.2020.00239

Yang Y, Wang G, Xie S (2012) Effect of magnesium sulfate on the unconfined compressive strength of cement-treated soils. *Journal of Testing and Evaluation* 40(7):1244-1251, DOI: 10.1520/JTE20120132

Yao K, An D, Wang W, Li N, Zhang C, Zhou A (2020) Effect of nano-MgO on mechanical performance of cement stabilized silty clay. *Marine Georesources & Geotechnology* 38(2):250-255, DOI: 10.1080/1064119X.2018.1564406

Yu C, Wang H, Zhou A, Cai X, Wu Z (2019) Experimental study on strength and microstructure of cemented soil with different suctions. *Journal of Materials in Civil Engineering* 31(6):04019082, DOI: 10.1061/(ASCE)MT.1943-5533.0002717

Yu D, Ye J, Yao L (2020) Prediction of the long-term settlement of the structures built on a reclaimed coral reef island: An aircraft runway. *Bulletin of Engineering Geology and the Environment* 79(9):4549-4564, DOI: 10.1007/s10064-020-01866-z

Yu Xt, Chen D, Feng Jr, Zhang Y (2018) Behavior of mortar exposed to different exposure conditions of sulfate attack. *Ocean Engineering* 157:1-12, DOI: 10.1016/j.oceaneng.2018.03.017

Zhang N, Shen JS, Zhou A, Arulrajah A (2018) Tunneling induced geohazards in mylonitic rock faults with rich groundwater: A case study in Guangzhou. *Tunnelling and Underground Space Technology* 74: 262-272, DOI: 10.1016/j.tust.2017.12.021